Engineering plasmonic nanorod arrays for colon cancer marker detection

Engineering plasmonic nanorod arrays for colon cancer marker detection

Stephanie L. Dodson, Cuong Cao, Hamed Zaribafzadeh, Shuzhou Li, Qihua Xiong

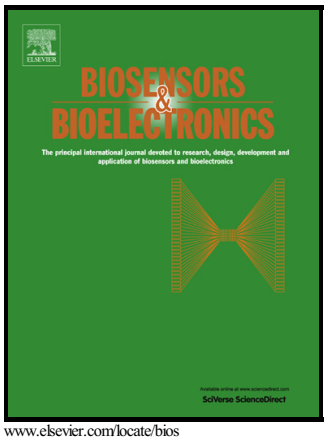

www.elsevier.com/locate/bios

PII: S0956-5663(14)00584-3
DOI: http://dx.doi.org/10.1016/j.bios.2014.07.083
Reference: BIOS6987

To appear in: *Biosensors and Bioelectronic*

Received date: 20 June 2014
Revised date: 28 July 2014
Accepted date: 30 July 2014

Cite this article as: Stephanie L. Dodson, Cuong Cao, Hamed Zaribafzadeh, Shuzhou Li and Qihua Xiong, Engineering plasmonic nanorod arrays for colon cancer marker detection, *Biosensors and Bioelectronic,* http://dx.doi.org/10.1016/j.bios.2014.07.083

Engineering Plasmonic Nanorod Arrays for Colon Cancer Marker Detection

Stephanie L. Dodson [a], Cuong Cao [b], Hamed Zaribafzadeh [a], Shuzhou Li [c], Qihua Xiong [a,d,*]

[a] Division of Physics and Applied Physics, School of Physical and Mathematical Sciences, Nanyang Technological University, Singapore 637371

[b]Institute for Global Food Security, School of Biological Sciences, Queen's University Belfast, Belfast BT9 5AG, United Kingdom;

[c] School of Materials Science and Engineering, Nanyang Technological University, Singapore 637371

[d] NOVITAS, Nanoelectronics Centre of Excellence, School of Electrical and Electronic Engineering, Nanyang Technological University, Singapore 639798

*Corresponding author: 21 Nanyang Link, SPMS-PAP-04-14, Singapore 637371; Tel: +65 65138495; Fax: +65 67957981; E-mail address: qihua@ntu.edu.sg.

Abstract

Engineering plasmonic nanomaterials or nanostructures towards ultrasensitive biosensing for disease markers or pathogens is of high importance. Here we demonstrate a systematic approach to tailor effective plasmonic nanorod arrays by combining both comprehensive numerical discrete dipole approximations (DDA) simulation and transmission spectroscopy experiments. The results indicate that 200 × 50 nm nanorod arrays with 300 × 500 nm period provide the highest FOM of 2.4 and a sensitivity of 310 nm/RIU. Furthermore, we demonstrate the use of nanorod arrays for the detection of single nucleotide polymorphism in codon 12 of the K-*ras* gene that are frequently occurring in early stages of colon cancer, with a sensitivity down to 10 nM in the presence of 100-fold higher concentration of the homozygous genotypes. Our work shows significant potential of nanorod arrays towards point-of-care applications in diagnosis and clinical studies.

Keywords

Plasmonics, nanorod array, localized surface plasmon resonance, biosensing, discrete dipole approximation, single nucleotide polymorphism

1. Introduction

Recently, we have witnessed considerable efforts for the development of plasmonics and photonics-based nanosensors for biochemical and genetic analysis, especially for screening and rapid detection of cancer markers (Anker et al. 2008; Cao et al. 2013; Chao and Guo 2003; de la Rica and Stevens 2012; Fan et al. 2010; Hao et al. 2008; Luk'yanchuk et al. 2010; Miroshnichenko et al. 2010; Peng et al. 2013; Rodriguez-Lorenzo et al. 2012; Truong et al. 2011; Verellen et al. 2009; Wen et al. 2013; Xu et al. 2011; Zhang et al. 2013). These systems provide a range of benefits such as shorter analysis time, lower consumption of sample, chemical reagent and energy, lower cost, and portability. Towards this end, the usage of the dielectric sensitivity of localized surface plasmon resonances (LSPR) of nanoparticles has been shown to be particularly robust and very sensitive to changes in the dielectric environment of surrounding (Dahlin et al. 2006; Haes et al. 2005; Willets and Van Duyne 2007; Yonzon et al. 2005). LSPR sensors have been reported to have sensitivities from 25 to 868 nm/RIU, depending on various substrate parameters (Jeong et al. 2013; Yeom et al. 2013). The effects of periodicity, geometry, polarization, and dielectric environment have been explored for tuning the LSPR responses of nanosphere, trianglular nanoprism, nanorods, *etc*. Highly sensitive LSPR biosensing has been done using the various plasmonic substrates (Chen et al. 2011; Homola 2008; Mayer and Hafner 2011; Stewart et al. 2008; Willets and Van Duyne 2007). LSPR-based sensing of DNA hybridization reached the attomolar scale, antibody-antigen binding has been detected at 2 pg/mL, and thrombin has been detected at concentrations of 1 ng/mL (Fong and Yung 2013; Guo and Kim 2012; Jeong et al. 2013; Tang et al. 2013; Yeom et al. 2013). Among these substrates, the nanorods possess outstanding plasmonic and photonic properties, exhibiting intrinsic transverse and longitudinal modes. The longitudinal mode of nanorods has been shown to be

sensitive to changes in refractive index and has the potential for high figure of merit (FOM) values. More importantly, bandwidth and the LSPR sensitivity of the AuNRs can be optimized by tuning their aspect ratios. One- and two-dimensional arrays of nanoparticles have been previously studied for their plasmonic resonances and longer wavelength photonic resonances (Ausman et al. 2012; Halas et al. 2011; Liu et al. 2011; Malynych and Chumanov 2003; Zou et al. 2004; Zou and Schatz 2004, 2006). Arrays of gold nanorods showed very sharp resonances that shifted significantly with variations in array parameters. Classical mechanics has been found to be sufficient to describe a system of nanoscale particles in arrays on the order of a wavelength of visible light, for instance, one of the versatile framework is the discrete dipole approximations (DDA) that has been used to study the classical electrodynamics of such a system (Chen et al. 2010; Lombardi and Birke 2009; Morton et al. 2011). Previously, DDA simulations of rectangular nanorod arrays showed the appearance of sharp photonic resonances in the near infrared (Ausman et al. 2012), which have not been experimentally identified.

In this work, nanorod arrays were studied for their plasmonic and photonic resonances and their potential as LSPR biosensing substrates. The plasmonic and photonic modes of gold nanorod arrays were studied through rigorous experiments and DDA simulation to observe their extinction efficiency spectra and electric near field. Rigorous periodicity studies were carried out to fully understand the behavior of photonic resonances resulting from the array structure. Upon the engineering and optimization of nanorod array, we have successfully used the AuNR array device as a plasmonic nanosensor for the detection of single nucleotide polymorphisms (SNPs) in codon 12 of the K-*ras* gene that are frequently occurring in early stages of colon cancer - the third most common type of human cancer today and the second most common cause of cancer related deaths (Hadley et al. 2004; Jemal et al. 2007).

2. Results and discussion

2.1 Nanorod Resonance Engineering

In order to understand the effects of changes in nanorod size and aspect ratio, the discrete dipole approximation (DDA) was used to simulate the extinction spectra of varying nanorod geometries (refer to supplementary information for full detail of simulation). This is an important factor to consider, as small variations in the fabrication procedure can drastically affect the experimental particle shape, which determines the LSPR properties. Fig. 1a shows the variation in resonance of a single nanorod with a constant length and varying width. Spectra for both polarizations are shown, longitudinal (parallel to the nanorod axis) and transverse (perpendicular to the nanorod axis). Fig. 1b shows the extinction spectra of a single nanorod with a constant width but varying length. There is very little variation in transverse resonance position for either variation in aspect ratio, though there is a slight red shift for an increase in nanorod thickness. The variation of aspect ratio, the length over the width of the particle, has a dramatic effect on the longitudinal resonance mode. Tuning the aspect ratio from 2.7 to 8 varies the resonance from 900 to 1400 nm. As the aspect ratio of the rod decreases, it becomes more sphere-like, in geometry and resonance.

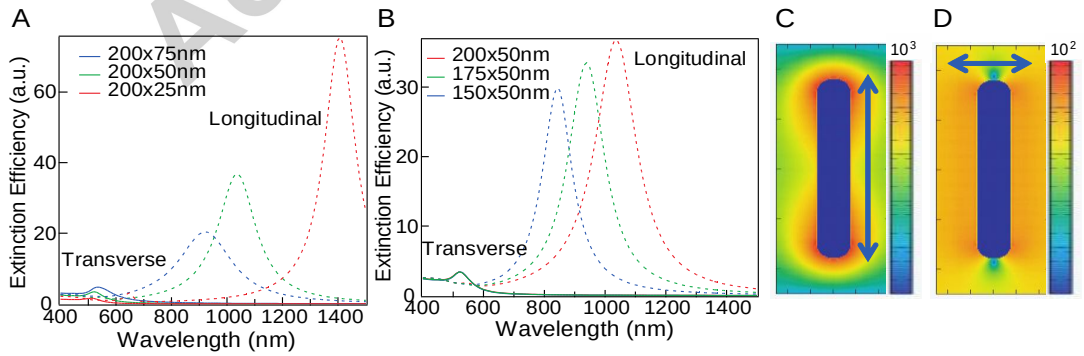

Fig. 1. Simulated extinction and electric field of nanorods. Simulated extinction efficiency of single nanorods with varying (a) widths and (b) lengths. Simulated electric near-field for single 200×50 nm nanorods with (c) longitudinal and (d) transverse polarization, demonstrated by the blue arrows.

To better understand the two modes, the electric near-field was computed. Fig. 1c and d show the electric near-field contour plots of a single nanorod with longitudinal and transverse polarizations, respectively. The longitudinal mode has hotspots located at the ends of the nanorod. The transverse mode has a more uniform electric near-field with cold spots at both ends of the nanorod. The weak electric field excited in the transverse mode will have weak interactions when particles are arranged in arrays. Changes in transverse periodicity may not make much impact on LSPR. The strong, localized electric field excited in the longitudinal mode, however, will interact strongly and changes in longitudinal periodicity will greatly affect the LSPR. It is noteworthy to comment that the local electric field contour can be directly visualized by near-field technique or indirectly mapped atomic force microscopy approaches, in which specific photosensitive polymers can be used to produce topographic variations due to conformational changes upon light irradiation (Dodson et al. 2013; Girard et al. 2000; Haggui et al. 2012; Hsu 2001; Hubert et al. 2008; Wiederrecht et al. 2005; Wurtz et al. 2003).

2.2 Nanorod Array Engineering: Effects of One Dimensional Arrays

In order to understand how periodicity affects the LSPR, it is necessary to first understand the effects of the two basic types of one-dimensional arrays. Fig. 2 shows the simulated extinction efficiency spectra for a single 200×50 nm nanorod and one-dimensional arrays, for transverse and longitudinal polarizations. Very large period arrays have similar LSPR to a single nanorod, since the particles are far enough apart that coupling is negligible. However,

as the period is decreased, and the near field of the particles can interact, the resonance shifts and new features appear. The near field excited in the transverse mode of nanorods does not interact in longitudinal arrays, therefore variation of periodicity in longitudinal arrays did not affect the transverse mode LSPR, as shown in Fig. 2a. The hotspots excited in longitudinal mode of nanorods interact strongly in longitudinal arrays and the longitudinal LSPR was greatly affected by changes in longitudinal periodicity, as shown in Fig. 2b. The appearance of a new peak around 1200 nm in the arrays with 500 and 1000 nm periodicities with longitudinal polarization warranted further studies, and Fig. 2c shows the extinction efficiency of a thorough study of the effect of periodicity in one-dimensional longitudinal arrays with longitudinal polarization. The appearance and subsequent red shift of two peaks is observed. These peaks appear very narrow and red shift and broaden until at their maximum extinction at approximately 830 and 415 nm periods. These values correspond roughly to the LSPR wavelength divided by the refractive index of the surrounding medium, 1.331 (divided by two for the 415 nm period). Fig. 2d and e show the extinction efficiency spectra of a single nanorod and various one-dimensional transverse arrays with transverse and longitudinal polarizations, respectively. There is comparatively little shift in the either resonance position for variations in the transverse periodicity, except when the particles are brought very close together. The longitudinal mode blue shifts as the periodicity decreased and the transverse mode red shifts with decreasing periodicity.

The red shift of the longitudinal mode in Fig. 2b and c implies that the electric near field of the longitudinal mode would be affected by changes in longitudinal periodicity. Also, the blue shift in Fig. 2e implies that the electric field intensity of the longitudinal mode will increase with decreasing transverse periodicity. Fig. 2f shows the simulated maximum electric field intensity

for a single nanorod and a variety of one-dimensional arrays with longitudinal polarization. Large period arrays of both types more closely resemble the single nanorod, as expected from similar results with the resonances. As the transverse period is decreased, the electric field increases. As the longitudinal periodicity is decreased the electric field intensity decreases. This result agrees with the patterns observed in the resonance shifts of both types of arrays.

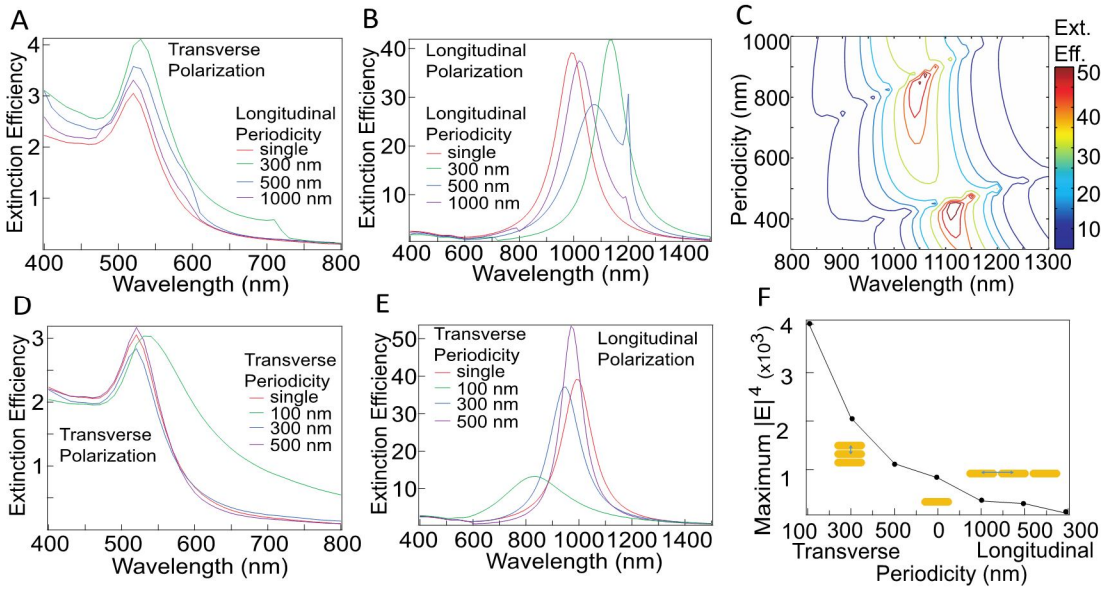

Fig. 2. Simulated extinction and electric field of one-dimensional nanorod arrays. (a-e) Simulated extinction efficiency spectra for one dimensional arrays of nanorods with: (a) longitudinal array with a transverse polarization; (b) longitudinal array with a longitudinal polarization; (c) further calculations of the longitudinal array with longitudinal polarization to follow the development of the peak formation; (d) transverse array with a transverse polarization; (e) transverse array with a longitudinal polarization. (f) Maximum electric field intensity for varying transverse and longitudinal one dimensional arrays as compared to a single nanorod, all with longitudinal polarization and 785 nm excitation.

2.3 Nanorod Array Engineering: Effects of Two Dimensional Arrays

After understanding the trends developed when nanorods are introduced into one-dimensional arrays, it is necessary to expand the system to two-dimensional arrays. Simulated spectra of two-dimensional arrays are of interest to compare with, and to better understand, potential experimental conditions. Fig. SI-1 shows the simulated extinction efficiency spectra of a variety of two-dimensional arrays. The longitudinal plasmonic mode, around 1000 nm, remains stationary with increasing transverse periodicity. There is a second longitudinal peak, around 1250 nm, which also remains stationary but undergoes sharpening with increased transverse periodicity. An increase in longitudinal array periodicity causes a blue shift in the plasmonic mode. The appearance and sharpening of the photonic resonance is more dramatic in the variation of the longitudinal periodicity.

2.4 Dielectric Sensitivity Testing

The sharp photonic resonances seen in simulation have great potential for biosensing, due to the narrow FWHM and high FOM, and so it was of great interest to demonstrate such resonances experimentally. This requires very high quality fabrication, in order to minimize the surface roughness effects and maintain consistent nanorod shape. In order to have a LSPR in the NIR with a high FOM, nanorods with 200 nm length and 50 nm width were chosen based upon simulation and fabricated by electron beam lithography (EBL), as shown in Fig. 3a. Full detail of the EBL fabrication can be found in the supplementary information. The uniform rod surface and defect-free structure integrity manifest the high quality of nanofabrication. Rectangular arrays were fabricated with periodicities varying from 100 nm to 1 μm in order to observe experimental effects of array parameters. Fig. 3b and c show the experimental transmission spectra of two-dimensional arrays with varying transverse and longitudinal periodicity, measured by a UV-Vis-IR microspectrophotometer (supplementary information). Increasing the longitudinal periodicity

blue shifts the longitudinal mode of the transmission spectra, in good agreement with simulation. Increasing the transverse periodicity red shifts the longitudinal mode of the transmission spectra, as predicted from the one-dimensional simulations. In the experimental transmission spectra the longitudinal mode of the 1000×100 nm array is red shifted from the resonance position predicted by the trend of the other two arrays, and the transverse mode is blue shifted. According to the study on nanorod geometry, shown in Fig. 1, both of these shifts implies that the nanorods in the 1000×100 nm array are wider than the nanorods in the other two arrays. This is likely due to overexposure of the PMMA resist during the EBL process since the nanorod pitch is so small in this array, demonstrating the important of high quality fabrication. The appearance of the sharp photonic resonance in the near-infrared region of the spectrum did not occur as expected from simulated results. This is assumed to be due to the dielectric mismatch of the experimental system. The simulated environment is a constant dielectric medium with refractive index of 1.331, whereas the experimental system consists of an indium-tin oxide (ITO) coated glass substrate and air. A dielectric medium with refractive index of 1.331 was determined to be the closest approximation to the experimental system, as the resonances match at these conditions.

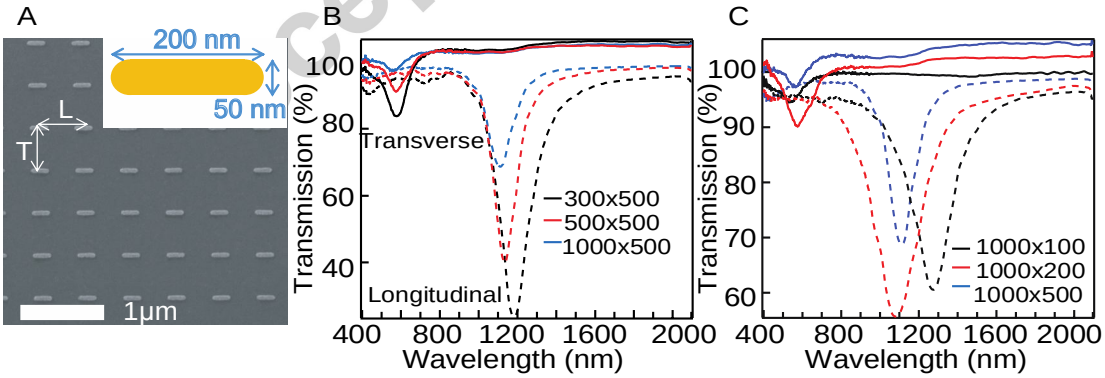

Fig. 3. (a) Scanning electron microscopy image of nanorod array. “L” denotes the longitudinal array parameter. “T” denotes the transverse array parameter. Inset shows the nanorod geometry.

Nanorods are 200 nm long and 50 nm wide. Experimental transmission spectra for two-dimensional nanorod arrays with varying (b) longitudinal and (c) transverse periodicity. In (b) and (c) solid lines represent transverse polarization and dashed lines represent longitudinal polarization.

An example of such a sharp resonance is evident in the 300 × 500 nm and 500 × 500 nm arrays. These arrays are instantly recognizable as potential LSPR biosensors as their narrow FWHM would result in a high FOM, meaning that very small shifts in the resonance easily distinguishable. To determine the sensitivity and FOM of this nanorod array, media of different refractive indices were applied and the resonance red shifts were measured. Fig. 4a shows, in black, the experimental sensitivity, 309.6 nm/RIU, of the longitudinal mode of a 300 × 500 nm array in a variety of concentrations of glycerol (supplementary information). The FWHM of this array was calculated to be 130 nm and from this the FOM was calculated to be 2.4. Fig. 4a also shows, in blue, the simulated sensitivity, 679.3 nm/RIU, of a single nanorod to changes in homogenous dielectric environment. Both calculations of the response of the system to changes in refractive index show a very good linear fit with a coefficient of determination very close to one. The discrepancy in sensitivity is due to the difference in nanoparticle surface area exposed to changes in dielectric material resulting from simulating a homogenous dielectric environment while the experimental conditions of a nanoparticle on an ITO/glass substrate coated with dielectric material. When considering that, using the effective medium theory, an ITO/glass substrate can be approximated in DDSCAT by a refractive index of 1.331, one could recalculate the simulated sensitivity, with adjusted refractive index to take the substrate into account. The simulated environment of a nanoparticle in a homogenous dielectric medium of refractive index 1.331 is equivalent to a particle on an ITO substrate in air. The simulated environment of a

nanoparticle in a homogenous dielectric medium of refractive index 1.5 is equivalent to a particle on an ITO substrate in a medium of RI 1.34. Using these equivalencies, a 126.6 nm shift for a change of medium with a refractive index of 0.34 RIU, the simulated sensitivity is 372.4 nm/RIU. This value is consistent with the experimental value.

2.5 Biosensing Limit of Detection Testing

In order to evaluate the sensitivity of the nanorod arrays as a potential biosensing platform, the shift caused by molecular binding events must be evaluated. We first chose to evaluate the response of the rod array device upon nucleic acid molecule binding. The nanorod array with the highest FOM was chosen, 300×500 nm period. Nanorod arrays were incubated sequentially with thiolated biotin, streptavidin, and biotinylated DNA, all in PBS buffer, and the LSPR shift was measured for each binding event. The full details of materials, DNA handling and manipulation can be found in supplementary information. Fig. 4b and c show the spectra and λ_{max} shifts, respectively, for different concentrations of biotinylated DNA, down to 0.1 aM. The spectral shift for 0.1 aM samples were poorly discriminated because their signals did not exceed 2 or 3 times of standard deviation from the blank measurement (PBS buffer), therefore the limit of detection (LOD) of biotinylated DNA detection was proposed to be approximately 10 fM. This is a very low limit of detection through streptavidin-biotin binding, and proves the potential of this plasmonic substrate as a biosensing platform towards ultrasensitive detection of nucleic acids.

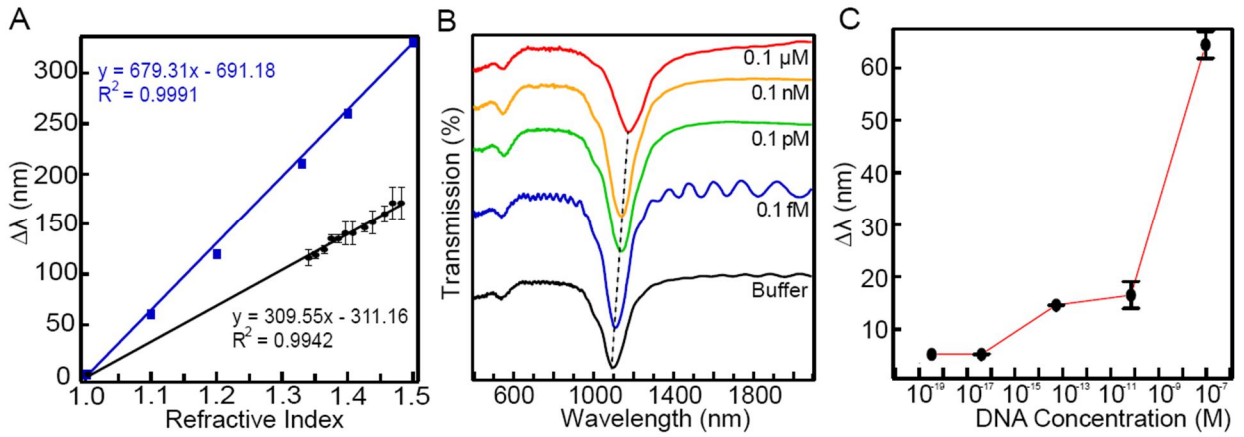

Fig. 4. LSPR-based chemical and biological sensing. (a) Dielectric sensitivity. Black data and equation denote the experimental study of a nanorod array on ITO/glass substrate with 300 nm longitudinal periodicity and 500 nm transverse periodicity coated with dielectric medium. Blue data and equation denotes the DDA simulation of a single nanorod in homogenous dielectric. (b) Spectra and (c) LSPR λ_{max} shift of the same nanorod array with varying concentrations of DNA in log scale.

2.6 Biosensing Detection of Single Nucleotide Polymorphism Detection

With an optimized performance in the near-infrared regime, nanorods array can be further devised as a high performance device towards the discrimination of single nucleotide polymorphism (SNP). As shown in Fig. 5a, the principle of the SNP detection is based on cleavage activity of SURVEYOR nuclease which has been shown to recognize and cleave all types of SNP in heteroduplex DNA with high specificity (Qiu et al. 2004). Following the immobilization of thiolated DNA probe molecules on the AuNRs surface, WT DNA or MT DNA containing SNP is introduced to bind with the DNA probe *via* DNA hybridization. SURVEYOR nuclease is subsequently applied to the AuNR arrays, leading to a specific cleavage of all imperfectly hybridized DNA duplexes (MT) while maintaining the perfectly hybridized

products with the WT DNA. The cleavage leads to shorter DNA molecules attached to the nanorods array, therefore the absorption bands blue shift. Fig. 5b and c represents consistent phase shifts caused by the molecular binding events. In both cases, wavelength red shifts after the DNA probe immobilization and after the DNA hybridization were respectively obtained about 20 nm and 51 nm as compared to the initial longitudinal plasmon band of the investigated AuNRs. Hybridization results with various WT DNA concentrations are shown in more detail in Fig. SI-2 which indicates that the AuNR arrays could be used to detect the DNA oligonucleotide at concentration as low as 2 nM. In addition, the enzymatic cleavage caused a tremendous blue-shift of about 45 nm in the case of 1 µM MT DNA, and this blue-shift value is only less than 9 nm in that of 1 µM WT which possibly corresponds to non-specific interaction between the WT DNA and the immobilized probes. To further investigate the discriminating power and selectivity of the assay, various ratio mixtures of MT/WT have been analyzed. As shown in the inset of Fig. 5c, the phase shift value is proportional to the increase of MT/WT ratios after the enzyme cleavage, and also exhibits good linearity ($R^2 = 0.97$). The detection limit of the enzyme cleavage assay is defined as three times the standard deviation for the average measurements of MT-free sample (0/1000), therefore the AuNRs sensor combined with the enzyme cleavage strategy could clearly discriminate the SNP down to 10 nM in the presence of 100-fold higher concentration of the WT DNA (MT/WT = 10/1000 nanomolar ratio).

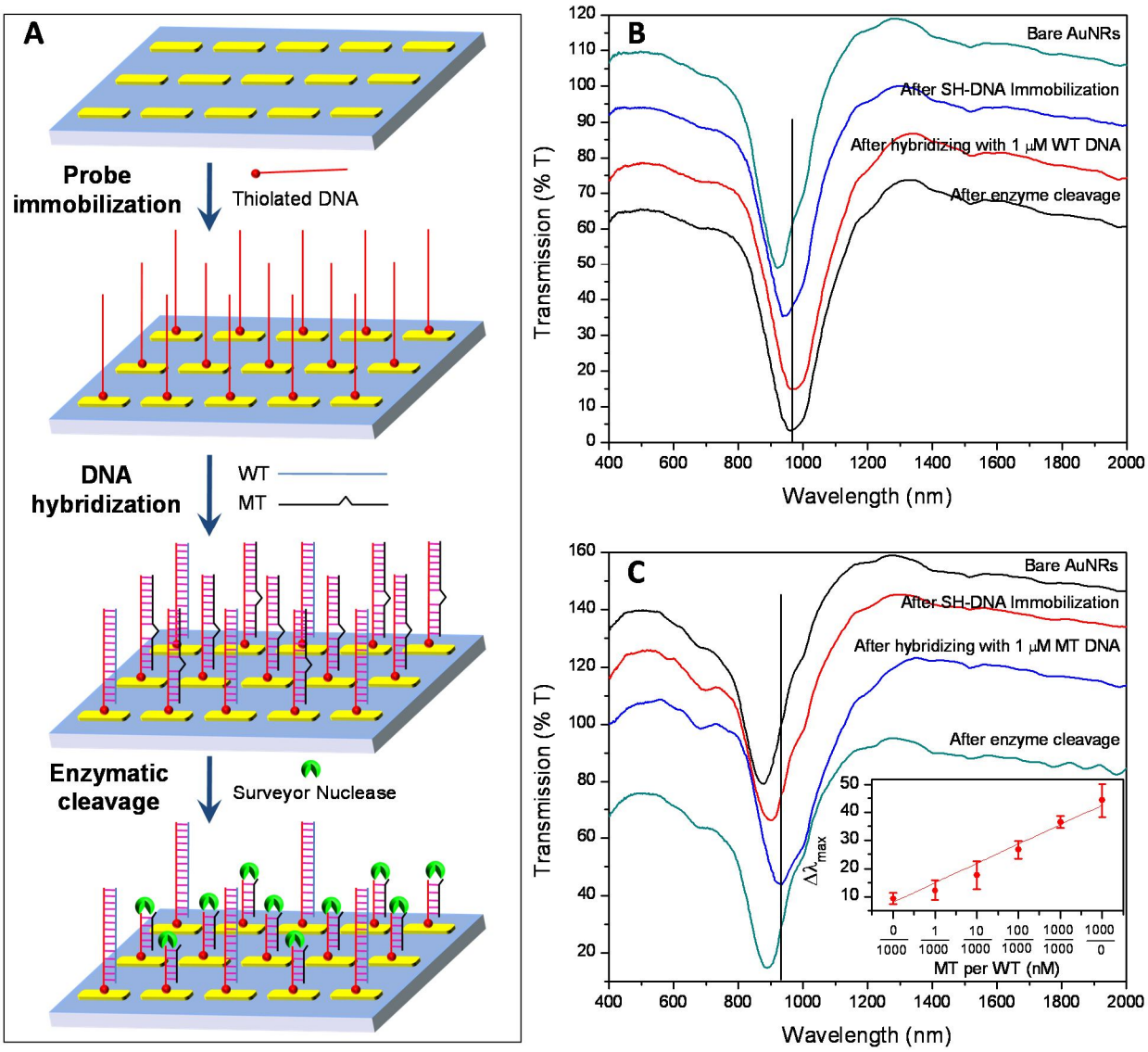

Fig. 5. Detection of single nucleotide polymorphism (SNP) by a means of AuNRs. (a). Overall scheme describing step-by-step procedure of the detection. (b). The enzymatic cleavage causes a very small blue-shift as hybridized with the WT DNA. (c) Transmission spectra under different scenario, indicating that a large blue-shift was obtained as hybridized with the MT DNA. Inset in Fig. C shows that the AuNRs sensor could clearly discriminate the SNP down to 10/1000 molar ratio of MT/WT.

3. Conclusions

In summary, we have systematically investigated the effects of nanorod geometry and array parameters in order to design an effective LSPR-based biosensing substrate. Increasing the aspect ratio of nanorods leads to sharpening of resonances and better FOM. Simulations of two-dimensional arrays, confirmed experimentally, have shown that increasing the longitudinal or transverse period blue shifts the longitudinal plasmonic resonance. No experimental evidence was found for the appearance of the photonic resonance shown in simulations. Lithographically fabricated nanorod arrays with very sharp resonances have proven to be highly sensitive to the surrounding refractive index, generating an effective LSPR substrate with a figure of merit of 2.4 and a sensitivity of 310 nm/RIU. DNA molecules were detected down to 10 fM. Colon cancer SNPs were detected down to 10/1000 molar ratio of MT/WT. The unambiguous discrimination of SNPs and the high sensitivity to local RI suggest that the nanorod arrays could be used for not only point mutation detections but also for a variety of applications such as cancer diagnostics and other point-of-care testing.

Acknowledgments

The author Q.X. would like to acknowledge the strong support from Singapore National Research Foundation through a Fellowship grant (NRF-RF2009-06) and a start-up grant support from Nanyang Technological University (M58110061). Q.X. and S.L. gratefully acknowledges the strong support from Singapore Ministry of Education via two Tier 2 grants (MOE2011-T2-2-051 and MOE2011-T2-2-085), respectively.

References

Anker, J.N., Hall, W.P., Lyandres, O., Shah, N.C., Zhao, J., Van Duyne, R.P., 2008. Biosensing with plasmonic nanosensors. Nature materials 7(6), 442-453.
Ausman, L.K., Li, S.Z., Schatz, G.C., 2012. Structural Effects in the Electromagnetic Enhancement Mechanism of Surface-Enhanced Raman Scattering: Dipole Reradiation and Rectangular Symmetry Effects for Nanoparticle Arrays. Journal of Physical Chemistry C 116(33), 17318-17327.
Cao, C., Zhang, J., Wen, X., Dodson, S.L., Dao, N.T., Wong, L.M., Wang, S., Li, S., Phan, A.T., Xiong, Q., 2013. Metamaterials-Based Label-Free Nanosensor for Conformation and Affinity Biosensing. ACS nano 7(9), 7583–7591.
Chao, C.Y., Guo, L.J., 2003. Biochemical sensors based on polymer microrings with sharp asymmetrical resonance. Applied Physics Letters 83(8), 1527-1529.
Chen, H.N., McMahon, J.M., Ratner, M.A., Schatz, G.C., 2010. Classical Electrodynamics Coupled to Quantum Mechanics for Calculation of Molecular Optical Properties: a RT-TDDFT/FDTD Approach. Journal of Physical Chemistry C 114(34), 14384-14392.
Chen, S., Svedendahl, M., Van Duyne, R.P., Kall, M., 2011. Plasmon-Enhanced Colorimetric ELISA with Single Molecule Sensitivity. Nano letters 11(4), 1826-1830.
Dahlin, A.B., Tegenfeldt, J.O., Hook, F., 2006. Improving the instrumental resolution of sensors based on localized surface plasmon resonance. Analytical Chemistry 78(13), 4416-4423.
de la Rica, R., Stevens, M.M., 2012. Plasmonic ELISA for the ultrasensitive detection of disease biomarkers with the naked eye. Nat Nanotechnol 7(12), 821-824.
Dodson, S., Haggui, M., Bachelot, R., Plain, J., Li, S.Z., Xiong, Q.H., 2013. Optimizing Electromagnetic Hotspots in Plasmonic Bowtie Nanoantennae. Journal of Physical Chemistry Letters 4(3), 496-501.
Fan, J.A., Wu, C.H., Bao, K., Bao, J.M., Bardhan, R., Halas, N.J., Manoharan, V.N., Nordlander, P., Shvets, G., Capasso, F., 2010. Self-Assembled Plasmonic Nanoparticle Clusters. Science 328(5982), 1135-1138.
Fong, K.E., Yung, L.Y.L., 2013. Localized surface plasmon resonance: a unique property of plasmonic nanoparticles for nucleic acid detection. Nanoscale 5(24), 12043-12071.
Girard, C., Joachim, C., Gauthier, S., 2000. The physics of the near-field. Rep Prog Phys 63(6), 893-938.
Guo, L.H., Kim, D.H., 2012. LSPR biomolecular assay with high sensitivity induced by aptamer-antigen-antibody sandwich complex. Biosensors & bioelectronics 31(1), 567-570.
Hadley, D.W., Jenkins, J.F., Dimond, E., de Carvalho, M., Kirsch, I., Palmer, C.G., 2004. Colon cancer screening practices after genetic counseling and testing for hereditary nonpolyposis colorectal cancer. Journal of clinical oncology : official journal of the American Society of Clinical Oncology 22(1), 39-44.
Haes, A.J., Chang, L., Klein, W.L., Van Duyne, R.P., 2005. Detection of a biomarker for Alzheimer's disease from synthetic and clinical samples using a nanoscale optical biosensor. J Am Chem Soc 127(7), 2264-2271.
Haggui, M., Dridi, M., Plain, J., Marguet, S., Perez, H., Schatz, G.C., Wiederrecht, G.P., Gray, S.K., Bachelot, R., 2012. Spatial Confinement of Electromagnetic Hot and Cold Spots in Gold Nanocubes. ACS nano 6(2), 1299-1307.
Halas, N.J., Lal, S., Chang, W.S., Link, S., Nordlander, P., 2011. Plasmons in Strongly Coupled Metallic Nanostructures. Chem Rev 111(6), 3913-3961.

Hao, F., Sonnefraud, Y., Van Dorpe, P., Maier, S.A., Halas, N.J., Nordlander, P., 2008. Symmetry Breaking in Plasmonic Nanocavities: Subradiant LSPR Sensing and a Tunable Fano Resonance. Nano letters 8(11), 3983-3988.
Homola, J., 2008. Surface plasmon resonance sensors for detection of chemical and biological species. Chem Rev 108(2), 462-493.
Hsu, J.W.P., 2001. Near-field scanning optical microscopy studies of electronic and photonic materials and devices. Mat Sci Eng R 33(1), 1-50.
Hubert, C., Bachelot, R., Plain, J., Kostcheev, S., Lerondel, G., Juan, M., Royer, P., Zou, S.L., Schatz, G.C., Wiederrecht, G.P., Gray, S.K., 2008. Near-field polarization effects in molecular-motion-induced photochemical imaging. Journal of Physical Chemistry C 112(11), 4111-4116.
Jemal, A., Siegel, R., Ward, E., Murray, T., Xu, J., Thun, M.J., 2007. Cancer statistics, 2007. CA: a cancer journal for clinicians 57(1), 43-66.
Jeong, H.H., Erdene, N., Park, J.H., Jeong, D.H., Lee, H.Y., Lee, S.K., 2013. Real-time label-free immunoassay of interferon-gamma and prostate-specific antigen using a Fiber-Optic Localized Surface Plasmon Resonance sensor. Biosensors & bioelectronics 39(1), 346-351.
Liu, N., Hentschel, M., Weiss, T., Alivisatos, A.P., Giessen, H., 2011. Three-Dimensional Plasmon Rulers. Science 332(6036), 1407-1410.
Lombardi, J.R., Birke, R.L., 2009. A Unified View of Surface-Enhanced Raman Scattering. Accounts of Chemical Research 42(6), 734-742.
Luk'yanchuk, B., Zheludev, N.I., Maier, S.A., Halas, N.J., Nordlander, P., Giessen, H., Chong, C.T., 2010. The Fano resonance in plasmonic nanostructures and metamaterials. Nature materials 9(9), 707-715.
Malynych, S., Chumanov, G., 2003. Light-induced coherent interactions between silver nanoparticles in two-dimensional arrays. J Am Chem Soc 125(10), 2896-2898.
Mayer, K.M., Hafner, J.H., 2011. Localized Surface Plasmon Resonance Sensors. Chem Rev 111(6), 3828-3857.
Miroshnichenko, A.E., Flach, S., Kivshar, Y.S., 2010. Fano resonances in nanoscale structures. Reviews of Modern Physics 82(3), 2257-2298.
Morton, S.M., Silverstein, D.W., Jensen, L., 2011. Theoretical Studies of Plasmonics using Electronic Structure Methods. Chem Rev 111(6), 3962-3994.
Peng, B., Li, G., Li, D., Dodson, S., Zhang, Q., Zhang, J., Lee, Y.H., Demir, H.V., Ling, X.Y., Xiong, Q., 2013. Vertically aligned gold nanorod monolayer on arbitrary substrates: self-assembly and femtomolar detection of food contaminants. ACS nano 7(7), 5993-6000.
Qiu, P., Shandilya, H., D'Alessio, J.M., O'Connor, K., Durocher, J., Gerard, G.F., 2004. Mutation detection using Surveyor nuclease. BioTechniques 36(4), 702-707.
Rodriguez-Lorenzo, L., de la Rica, R., Alvarez-Puebla, R.A., Liz-Marzan, L.M., Stevens, M.M., 2012. Plasmonic nanosensors with inverse sensitivity by means of enzyme-guided crystal growth. Nature materials 11(7), 604-607.
Stewart, M.E., Anderton, C.R., Thompson, L.B., Maria, J., Gray, S.K., Rogers, J.A., Nuzzo, R.G., 2008. Nanostructured plasmonic sensors. Chem Rev 108(2), 494-521.
Tang, L., Casas, J., Venkataramasubramani, M., 2013. Magnetic Nanoparticle Mediated Enhancement of Localized Surface Plasmon Resonance for Ultrasensitive Bioanalytical Assay in Human Blood Plasma. Analytical Chemistry 85(3), 1431-1439.
Truong, P.L., Cao, C., Park, S., Kim, M., Sim, S.J., 2011. A new method for non-labeling attomolar detection of diseases based on an individual gold nanorod immunosensor. Lab on a chip 11(15), 2591-2597.

Verellen, N., Sonnefraud, Y., Sobhani, H., Hao, F., Moshchalkov, V.V., Van Dorpe, P., Nordlander, P., Maier, S.A., 2009. Fano Resonances in Individual Coherent Plasmonic Nanocavities. Nano letters 9(4), 1663-1667.
Wen, X., Li, G., Zhang, J., Zhang, Q., Peng, B., Wong, L.M., Wang, S., Xiong, Q., 2013. Transparent free-standing metamaterials and their applications in surface-enhanced Raman scattering. Nanoscale 6, 132-139.
Wiederrecht, G.P., Wurtz, G.A., Hranisavljevic, J., 2005. Near-field scanning optical microscopy of metal nanoparticles and nanoscale heterostructures. Abstracts of Papers of the American Chemical Society 229, U865-U865.
Willets, K.A., Van Duyne, R.P., 2007. Localized surface plasmon resonance spectroscopy and sensing. Annu Rev Phys Chem 58, 267-297.
Wurtz, G.A., Hranisavljevic, J., Wiederrecht, G.P., 2003. Electromagnetic scattering pathways for metallic nanoparticles: A near-field optical study. Nano letters 3(11), 1511-1516.
Xu, X.L., Peng, B., Li, D.H., Zhang, J., Wong, L.M., Zhang, Q., Wang, S.J., Xiong, Q.H., 2011. Flexible Visible-Infrared Metamaterials and Their Applications in Highly Sensitive Chemical and Biological Sensing. Nano letters 11(8), 3232-3238.
Yeom, S.H., Han, M.E., Kang, B.H., Kim, K.J., Yuan, H., Eum, N.S., Kang, S.W., 2013. Enhancement of the sensitivity of LSPR-based CRP immunosensors by Au nanoparticle antibody conjugation. Sensors and Actuators B-Chemical 177, 376-383.
Yonzon, C.R., Stuart, D.A., Zhang, X.Y., McFarland, A.D., Haynes, C.L., Van Duyne, R.P., 2005. Towards advanced chemical and biological nanosensors - An overview. Talanta 67(3), 438-448.
Zhang, Q., Wen, X., Li, G., Ruan, Q., Wang, J., Xiong, Q., 2013. Multiple Magnetic Mode-Based Fano Resonance in Split-Ring Resonator/Disk Nanocavities. ACS nano 7(12), 11071–11078.
Zou, S.L., Janel, N., Schatz, G.C., 2004. Silver nanoparticle array structures that produce remarkably narrow plasmon lineshapes. J Chem Phys 120(23), 10871-10875.
Zou, S.L., Schatz, G.C., 2004. Narrow plasmonic/photonic extinction and scattering line shapes for one and two dimensional silver nanoparticle arrays. J Chem Phys 121(24), 12606-12612.
Zou, S.L., Schatz, G.C., 2006. Coupled plasmonic plasmon/photonic resonance effects in SERS. Surface-Enhanced Raman Scattering: Physics and Applications 103, 67-85.